NANO LETTERS

Letter

pubs.acs.org/NanoLett

Plasmonic Coupling in Gold Nanoring Dimers: Observation of Coupled Bonding Mode

Chia-Yang Tsai, Jyun-Wei Lin, Che-Yao Wu, Pin-Tso Lin, Tsan-Wen Lu, and Po-Tsung Lee*

Department of Photonics and Institute of Electro-Optical Engineering, National Chiao Tung University, Room 415 CPT building, 1001 Ta-Hsueh Road, Hsinchu 300, Taiwan

Supporting Information

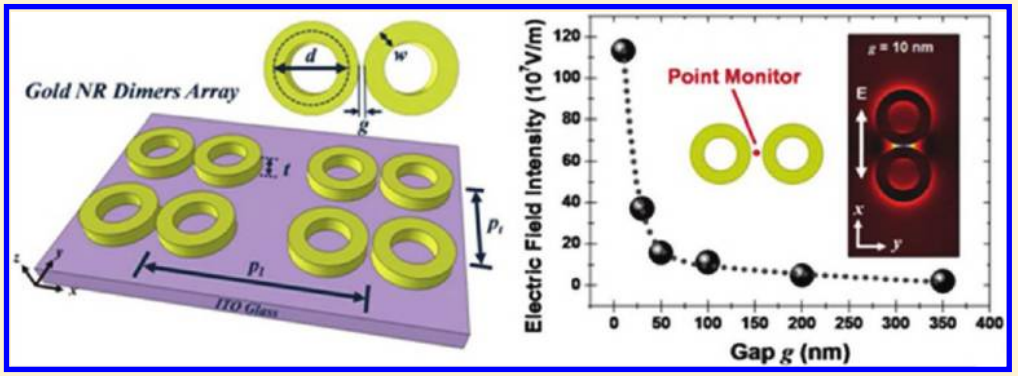

ABSTRACT: We investigate the optical properties of gold nanoring (NR) dimers in both simulation and experiment. The resonance peak wavelength of gold NR dimers is strongly dependent on the polarization direction and gap distance. As the gold NR particles approach each other, exponential red shift and slight blue shift of coupled bonding (CB) mode in gold NR dimers for longitudinal and transverse polarizations are obtained. In finite element method analysis, a very strong surface plasmon coupling in the gap region of gold NR dimers is observed, whose field intensity at the gap distance of 10 nm is enhanced 23% compared to that for gold nanodisk (ND) dimers with the same diameter. In addition, plasmonic dimer system exhibits a great improvement in the sensing performance. Near-field coupling in gold NR dimers causes exponential increase in sensitivity to refractive index of surrounding medium with decreasing the gap distance. Compared with coupled dipole mode in gold ND dimers, CB mode in gold NR dimers shows higher index sensitivity. This better index sensing performance is resulted form the additional electric field in inside region of NR and the larger field enhancement in the gap region owing to the stronger coupling of collective dipole plasmon resonances for CB mode. These results pave the way to design plasmonic nanostructures for practical applications that require coupled metallic nanoparticles with enhanced electric fields.

KEYWORDS: *Surface plasmon, plasmonic array, nanoring, dimers, index sensing*

Nanoscale light confinement and localization by noble metallic nanostructures is one of the critical aspects of nanophotonics. The plasmonic properties of metallic nanostructures are dominated by the oscillations of the free electrons of the nanostructure in resonance with the incident electromagnetic field. This so-called localized surface plasmon resonance (LSPR) results in a strongly enhanced electric near-field localized at the particle surface,[1,2] which has received enormous interest because of its potential for various technological applications such as optical waveguiding,[3] nanotrapping,[4] nonlinear optics,[5] and field enhancement spectroscopy.[6−9] During the past decade, a great number of investigations of coupled metallic nanoparticles including gold particle chains,[10] silver cube clusters,[11] gold disk trimers,[12] and gold necklaces[13] have been carried out to understand the plasmon coupling between metal nanoparticles. The local electric field enhancement resulted from the nearly adjacent two metallic particles is much larger than those associated with spatially isolated ones.[14] More importantly, the enhanced optical field confined in nanogap region of two adjacent nanoparticles can be used to monitor the response of LSPR to environmental change. This feature provides remarkable opportunities to improve single-molecule detection[15,16] and have profound significance for probing biochemistry including chemical reactions[17] and molecular bonding[18] to serve as a nanoreactor.

Coupled metallic nanoparticle pairs are referred to as plasmonic dimers, which give rise to very large field enhancements in their gap region because of the near-field coupling as two particles are close enough. Since the condition of LSPR oscillations is sensitively dependent on the geometry of the nanostructure, the control of particle shape for plasmonic dimers is a crucial issue, which can significantly influence the performance of field enhancement. Up to date, various types of

Received: January 2, 2012
Published: February 9, 2012

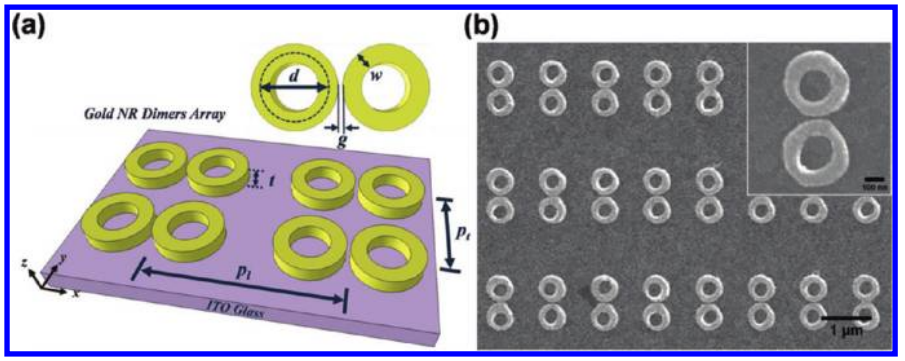

Figure 1. (a) Scheme of gold NR dimers array design. (b) SEM image of fabricated gold NR dimers array with w = 100 nm, d = 400 nm, g = 15 nm, t = 50 nm, p_l = 2 μm, and p_t = 1 μm. The inset shows a magnified SEM image of single gold NR dimer for the measurement of the gap distance.

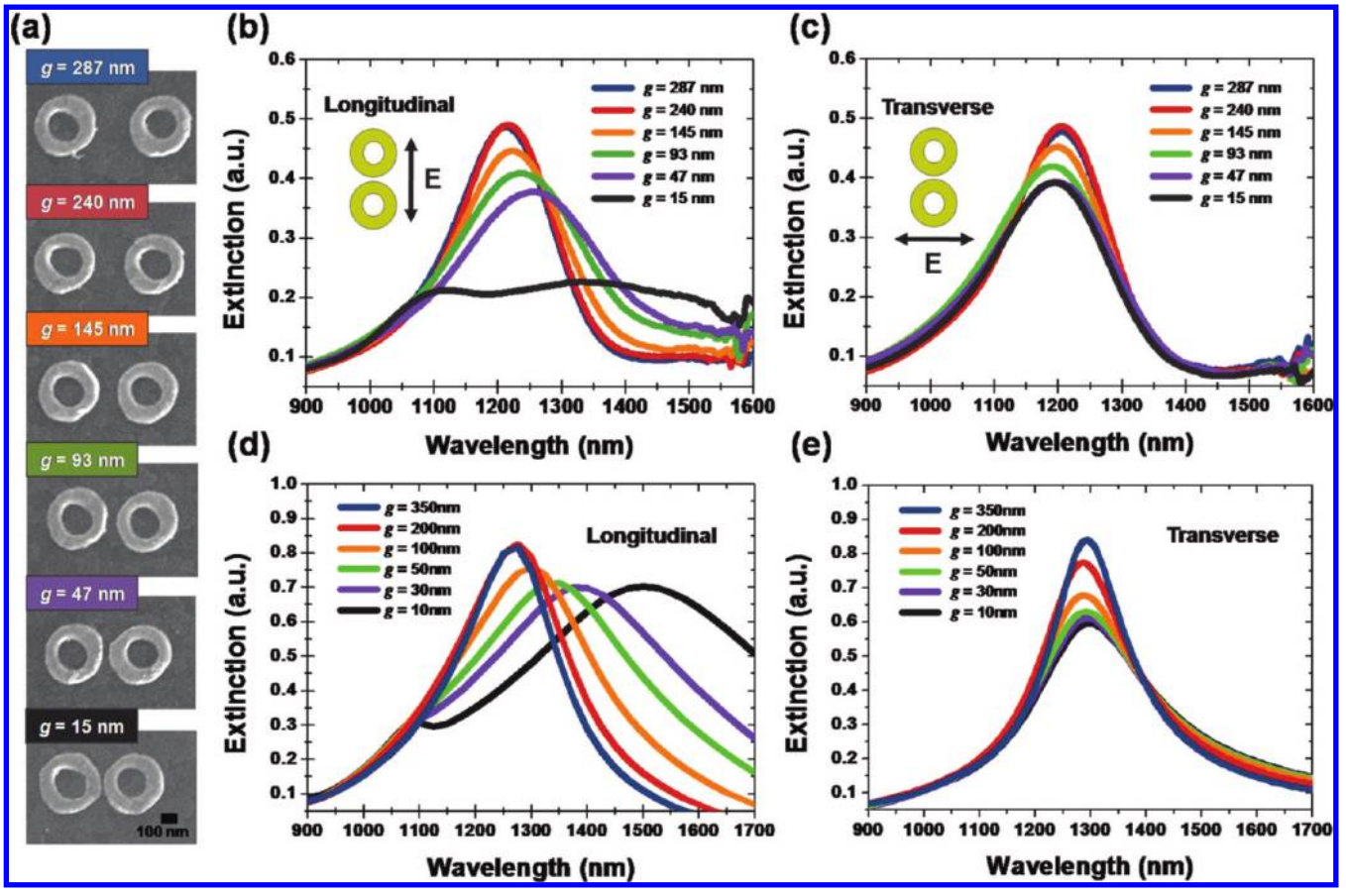

Figure 2. (a) SEM images of gold NR dimers with different gap distances within a range of 15−287 nm. (b,c) Measured and (d,e) simulated extinction spectra of gold NR dimers with different gap distances for (b,d) longitudinal and (c,e) transverse polarizations.

dimers structures have been investigated, such as circular and elliptical disk dimers,[19,20] nanoshell dimers,[21] nanorod dimers,[22] and triangular bowtie dimers.[23] In addition, to investigate the nanoantenna effect at the gap region, most previous studies have focused on its plasmon frequency and coupling strength tuning by varying the gap distance for incident light polarized perpendicular and parallel to the dimer axis.[24−26] When incident polarization is parallel to the dimer axis, an apparent exponential red shift of the plasmon resonance occurs with decreasing the separation of nanoparticles. However, a weak blue shift for perpendicular polarization is obtained. This highly gap-dependent behavior of collective plasmon modes has been theoretically demonstrated using plasmon hybridization model by many researchers.[27,28]

Recently, nanoring (NR) structures are particularly attractive since such structures produce high local electric field resulting from plasmons strongly coupled at the inner and outer surfaces. Furthermore, NR exhibits highly tunable plasmonic resonance from the visible to near-infrared (NIR) region by changing the dimension and width of the ring.[29,30] These properties of NR have been used widely in applications including surface-enhanced Raman scattering (SERS),[31] biosensing,[32] and plasmonic waveguide.[33] In general, the plasmon behaviors in NR structures can be explained by a simple universal physical model,[27,34] which has been vitally successful to describe the optical characteristics of other hybrid plasmonic nanostructures, such as nanoshells[35] and nanorice.[36] For NR structures, the plasmonic properties can be seen as the electromagnetic

dx.doi.org/10.1021/nl300012m | Nano Lett. 2012, 12, 1648−1654

interaction between the nanodisk (ND) and the nanohole plasmons.[37] This hybrid coupling leads to the splitting of the plasmon mode into two resonance modes, which are the low energy "bonding" mode and the high energy "antibonding" mode. However, bonding mode is preferred since the charge distribution of such mode can be regarded as a strong dipolar mode which strongly enhances the field intensity in NR.[29]

In this work, we present experimental and simulation investigations of the coupled bonding (CB) mode in gold NR dimers for different polarizations. The gap distance between two adjacent gold NR particles is systematically varied for probing the near-field interaction of CB modes. Moreover, to demonstrate the excellent plasmonic properties for gold NR dimers, optical behavior of typical coupled dipole (CD) mode in gold ND dimers with different gap distances are studied (see Supporting Information) and their sensing characteristics are also investigated for comparison. We show that index sensitivities of CB and CD modes in gold NR and ND dimers both exhibit an exponential relationship with gap distances. In particular, gold NR dimers have a significantly better sensing performance resulting from higher local field intensity in the gap region. This work can advance our understanding on the plasmon interactions between hybrid plasmonic nanostructures and greatly facilitate our abilities to design plasmonic nanoparticle dimers.

The scheme of gold NR dimers array with average ring width w, diameter d, gap distance g, thickness t, periods along the dimer axis p_l, and along the perpendicular direction p_t is shown in Figure 1a. In our fabrication, gold NR dimers arrays were manufactured on commercial indium tin oxide (ITO) glass substrate since conductive substrate can eliminate the charge accumulation effect during electron beam lithography (EBL). First, ITO glass substrate was cleaned by consecutive 5 min sonication cycles in acetone, isopropyl aclohol, and deionized water, after which the substrate was blown dry by N_2. The substrate was then spin-coated a 150 nm polymethylmethacrylate (PMMA) layer, and the NR dimers arrays consisting of 45 451 unit cells with dimensions of 300 × 300 μm^2 were defined on the PMMA layer by EBL. After the development process, the substrate was covered with a 50 nm gold thin film using thermal evaporation followed by a lift-off procedure (Supplementary Figure S1, Supporting Information). The average ring width w, diameter d, thickness t, periods p_l and p_t of fabricated gold NR dimers arrays are fixed at 100, 400, 50, 2000, and 1000 nm. Figure 1b shows a top-view scanning electron microscope (SEM) image of the fabricated gold NR dimers array with gap distance of 15 nm.

The extinction spectra of gold NR dimers arrays were measured using upright transmission spectroscopy with halogen lamp as a light source. Light was polarized and focused on gold NR dimers arrays through a linear polarizer and a 20× objective lens. The spot size was around 150 μm in diameter. The transmitted light was then collected by another 20× objective lens and fed into a multimode optical fiber connected to an optical spectrum analyzer (Supplementary Figure S2, Supporting Information). To investigate the influence of coupling effect on the optical behavior of CB mode, the gap distance g between two gold NR particles is varied. Figure 2a shows the SEM images of fabricated gold NR dimers with gap distances of 287, 240, 145, 93, 47, and 15 nm. Measured extinction spectra of gold NR dimers arrays with different gap distances are shown in Figure 2b,c. Two different polarization directions of the incident light were chosen. Longitudinal and transverse polarizations correspond to the polarization of incident light parallel and perpendicular to the NR dimers axis, as shown in the insets of Figure 2b,c. In the NIR spectral region, gold NR dimers exhibit a strong optical resonance that can be identified as the CB mode. The spectral behavior of CB mode is in strong disparity for different polarization directions. For the longitudinal polarization, the CB mode shows a considerable red shift as the gap distance of NR dimers is reduced. However, only very slight blue shift is obtained for transverse polarization. This polarization dependence of CB mode can be explained by a dipole−dipole coupling model[24,25,38] since bonding mode in gold NR structure can be regarded as a dipole mode from the charge distribution. Generally, when two plasmonic nanoparticles approach one another in dipole-dimers system for longitudinal polarization, the strengthened attractive force between two dipolar particles would weaken the repulsive forces within each particle, which results in the reduction of the plasmon frequency. On the contrary, two dipolar particles collectively enhance the repulsive forces for transverse polarization, which causes the growth of plasmon frequency. Additionally, the peak around 1100 nm for gold NR dimers with gap distance of 15 nm is evidently observed. This resonance mode is associated with the coupling of high-order quadrupole plasmon modes, which has also been investigated in previous work for gold ND dimers with nearly touching particles presented by Jain et al.[25]

To verify the effects of gap distance on peak wavelength for longitudinal and transverse polarizations, we calculated the extinction spectra of gold NR dimers with various gap distances using three-dimensional finite element method (FEM). In our simulation, the dielectric function of gold NR was described by the Lorenz−Drude model.[39] The dimensions of simulated NR structure were chosen to match those of fabricated NR. The gap distance of gold NR dimer was varied for a wide range from 10 to 350 nm to investigate the gap effect thoroughly. The refractive index of surrounding medium was set to be 1.0 for air and the dispersion of ITO substrate was considered. Figure 2d,e shows the simulated extinction spectra of gold NR dimers with different gap distances for longitudinal and transverse polarizations. With decreasing the gap distance, a strong red shift and a very weak blue shift are obtained for longitudinal and transverse polarizations. Moreover, under longitudinal polarization, a shoulder in the spectral range from 1050 to 1150 nm for extremely small gap distance is observed, which can be ascribed to high-order interactions. These features of the simulated results are clearly reproduced in our experiments. Furthermore, we show the measured and simulated extinction spectra of gold ND dimers with different gap distances for comparison (see Supporting Information for details). As expected, when two gold ND particles approach each other, red shift and blue shift of the extinction peaks associated with the CD mode as decreasing the gap distance are observed for longitudinal and transverse polarizations. The trends are analogous to those obtained for gold NR dimers with the same diameter.

To further investigate the peak wavelength shift trend for longitudinal polarization, the measured and simulated peak wavelengths of CB mode in gold NR dimers with different gap distances are plotted in Figure 3. The experimental observations are in good agreement with the simulation results, which both show the exponential red shifts of the plasmon resonance with decreasing gap distance. The measured peak resonances are at 1212, 1214, 1222, 1234, 1254, and 1335 nm

dx.doi.org/10.1021/nl300012m | Nano Lett. 2012, 12, 1648−1654

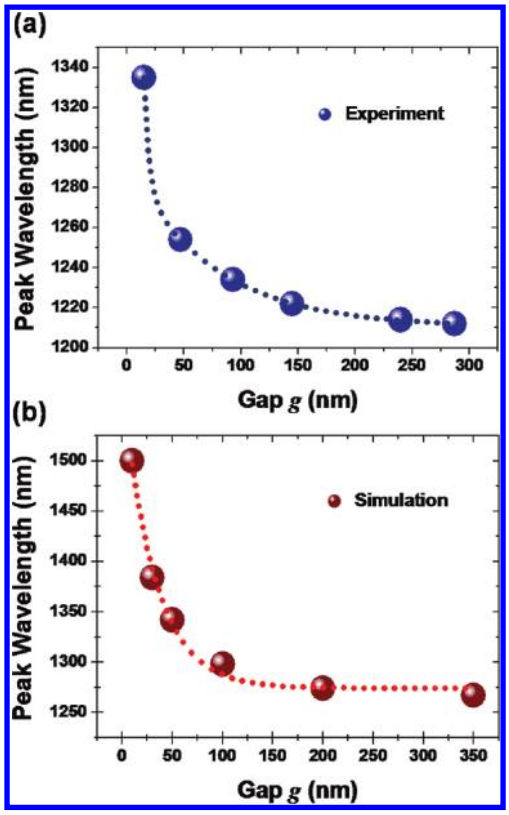

Figure 3. (a) Measured and (b) simulated peak wavelengths of CB mode in gold NR dimers with various gap distances *g* for longitudinal polarization. The dotted lines are the best-fit exponential decay function to the data.

for the gap distances of 287, 240, 145, 93, 47, and 15 nm. Also, the simulated peak resonances are at 1267, 1274, 1298, 1342, 1384, and 1500 nm for the gap distances of 350, 200, 100, 50, 30, and 10 nm. The larger gap distance causes the higher plasmon frequency because of the weaker coupling in plasmonic dimers. The peak wavelengths are slightly larger for simulation results since the idealized slab-like NR dimers with homogeneous sizes and gaps were assumed. This is deviated from the true experimental situation.

To confirm the CB and high-order CB modes in gold NR dimers, the near-field vector distributions in a horizontal plane are obtained. Figure 4a shows the simulated extinction spectra of gold NR dimers with gap distance of 10 nm for longitudinal and transverse polarizations, and the corresponding near-field vector distributions of resonance modes are shown in Figure 4b–d. The extinction spectrum for longitudinal polarization exhibits two well-defined peaks resulted from the strong coupling of bonding modes. Obviously, the electric field intensity is enhanced at the gap region of the gold NR dimers for longitudinal polarization. According to the electric field vector distributions, the sign of local surface charges can be defined by the directional arrows. For NR structure, the charge distributions of the bonding mode show the same signs at the inner and outer ring surfaces. Figure 4b,c shows a dipole–dipole-like charge pattern for the CB mode at 1500 nm and a quadrupole–quadrupole-like charge pattern for the high-order CB bonding mode at 1095 nm for longitudinal polarization. The CB mode at 1298 nm for transverse polarization also exhibits a dipole–dipole-like charge pattern, as shown in Figure 4d. However, there is no enhanced field in the gap region since

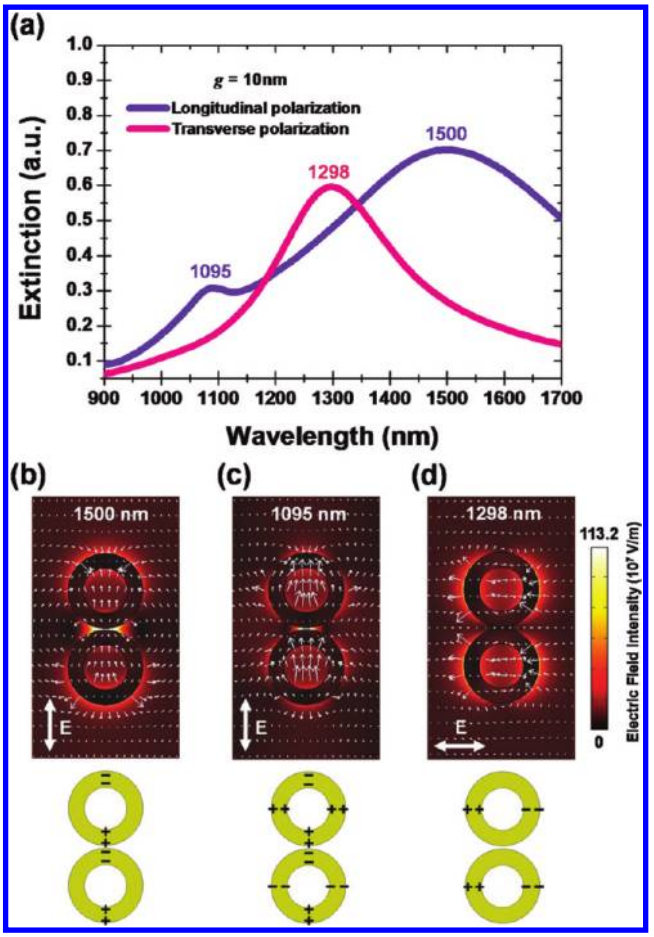

Figure 4. (a) Simulated extinction spectra of gold NR dimers with gap distance of 10 nm for longitudinal and transverse polarizations. Electric field intensity distributions with flux lines and the surface charge distributions of (b) CB mode, (c) high-order CB mode for longitudinal polarization, and (d) CB mode for transverse polarization in gold NR dimers with gap distance of 10 nm.

the surface charges are excited along the direction perpendicular to dimer axis.

Then we study the gap effect on electric field intensity distribution of the CB mode in gold NR dimers under longitudinal polarization. The field intensity distributions on top surface of gold NR dimers with different gap distances for longitudinal polarization are shown in Figure 5a. It is evident that when two adjacent gold NR particles come in close proximity, collective dipolar-like NR plasmons result in extremely enhanced fields in the gap region. The cross sections of the field intensity distributions along the dimer axis for gold NR dimers with different gap distances were displayed, as shown in Figure 5b. The strong near-fields are spatially concentrated in the gap region and the electric field intensity is significantly augmented as reducing the gap distance. The intensity of electric field at the center of gap region of the gold NR dimers as a function of gap distance was investigated, as shown in Figure 5c. The field intensity exponentially increases with decreasing gap distance for longitudinal polarization. When the gap distance is decreased from 350 to 10 nm, the intensity enhancement of around 60 times is obtained. Furthermore, the highest electric-filed intensity of 113.2×10^7 V/m at the gap center for gold NR dimers is 23% larger than that for gold ND dimers with identical size (see

dx.doi.org/10.1021/nl300012m | *Nano Lett.* 2012, 12, 1648–1654

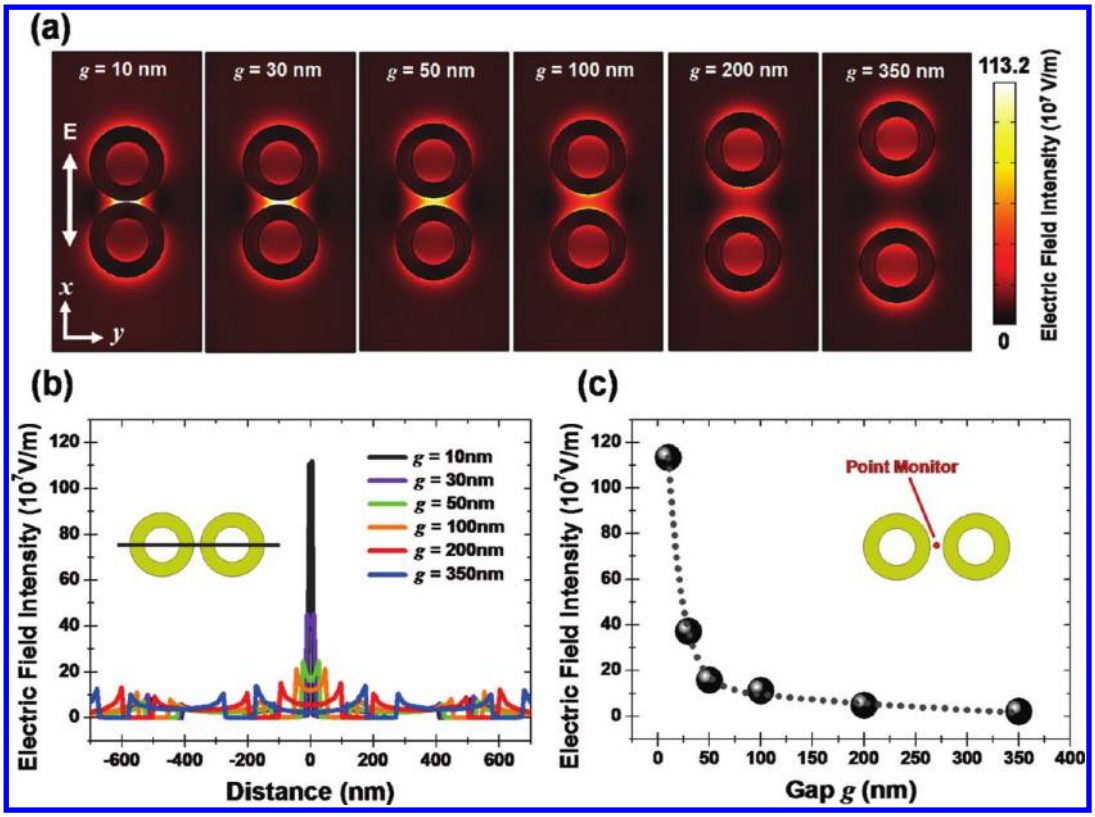

Figure 5. (a) Electric-field intensity distributions on top surface and (b) their cross sections along the solid black line of gold NR dimers with different gap distances for longitudinal polarization. (c) Electric-field intensity of the CB mode as a function of gap distance at the gap center (denoted by the point monitor) of gold NR dimers. The dotted line is the best-fit exponential decay function to the data.

Supporting Information) at the gap distance of 10 nm. This stronger enhancement of field intensity for gold NR dimers is attributed to the enhanced coupling for CB mode.

The LSPR is popularly known to be sensitive to the medium surrounding the metallic nanoparticle. Recently, the effect of the surrounding medium on the optical properties of noble metal nanostructures has attracted much attention and been utilized for chemical and biological sensing applications.[40−42] Several researches on the optical response of complex metallic nanoparticles to medium refractive index changes have been investigated.[36,43,44] However, the effect of the medium on the plasmon resonance coupling in dimers based on hybrid plasmonic nanoparticle has not been entirely elucidated. Thus, we continue by investigating the index sensitivity of gold NR dimers by varying the refractive index of the surrounding medium and comparing with gold ND dimers by simulations. For gold NR dimers with the gap distance of 10 nm, the peak wavelength of the CB mode shifts from 1500 to 1663 nm as refractive index of surrounding medium is increased from 1.00 to 1.15. A very high sensitivity of 1084 nm per refractive index unit (RIU) is obtained by calculating the slope of the peak fitting curve. In addition, the index sensitivities of both gold NR and ND dimers with different gap distances were studied. Figure 6 shows a plot of the simulated index sensitivities of the CB and CD modes in gold NR and ND dimers as a function of the gap distance. The sensitivities of gold NR and ND dimers significantly increase at a near-exponential rate with decreasing gap distance. We attribute the sensitivity enhancements in both dimers systems to electromagnetic coupling between the nanoparticles. For gold NR dimers, the index sensitivity is greatly enhanced from 547 to

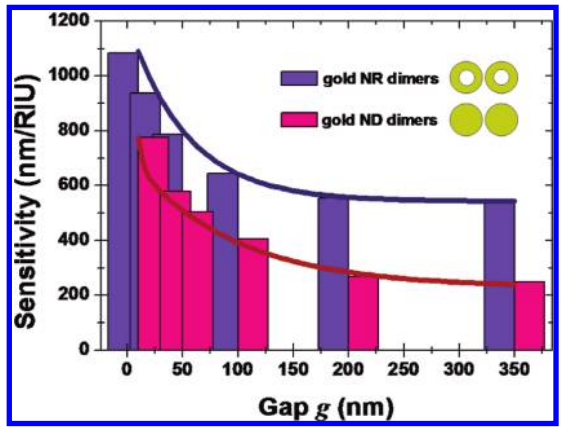

Figure 6. Simulated index sensitivities of the CB and CD modes in gold NR and ND dimers with different gap distances. Solid lines represent the fitting curves with exponential decay function.

1084 nm per RIU when the gap distance is reduced from 350 to 10 nm. Furthermore, the sensitivity of gold NR dimers is larger than that of gold ND dimers with the same gap distance. This phenomenon can be explained by the field intensity and distribution of plasmon resonance mode. Gold NR dimers exhibits larger field enhancement than gold ND dimers in the gap region because of the charge distribution of bonding mode. Moreover, unlike in ND structure, there is an electric field distributed in inside region of the NR structure, which is accessible to the environmental change, in turn making NR structure additional advantage for index sensing applications. Thus, compared to conventional solid metallic nanostructures such as sphere and disk dimers, our proposed sensitivity

dx.doi.org/10.1021/nl300012m | Nano Lett. 2012, 12, 1648−1654

enhancement in gold NR dimers suggests that CB mode in hybrid plasmonic nanostructure-based dimers is more suitable for LSPR sensing.

In summary, we have investigated the optical behavior of plasmon coupling and near-field localization properties for gold NR dimers with different gap distances in experiments and simulations. The peak wavelength of CB mode in gold NR dimers is strongly dependent on polarization direction. For longitudinal and transverse polarizations, the peak wavelengths show exponential increase and slight decrease respectively when gold NR particles approach each other. This phenomenon can be illustrated using dipolar-coupling model since the bonding mode in NR structure can be regarded as a dipolar-like mode. From the electric field intensity distribution, gold NR dimers exhibit increased field intensity in the gap region when decreasing the gap distance owing to near-field coupling. Compared to gold ND dimers with the same gap distance, gold NR dimers show a higher field intensity in the gap region resulted from the strong coupling of collective dipole plasmon resonances for CB mode. For index sensing, plasmon couplings in gold NR and ND dimers result in exponential sensitivity increase when reducing the gap distance. However, the index sensitivities of gold NR dimers are substantially larger than those of gold ND dimers with similar sizes. This results from larger field enhancement in the gap region for CB mode and additional sensing provided by the electric field in the inside region of NR for the detection of the environmental change. These results indicate that CB mode in gold NR dimers has a great potential and is highly attractive for many applications, such as chemical and biological sensor, field-enhanced spectroscopy, and nanoparticle trapping.

■ ASSOCIATED CONTENT

Supporting Information

Supporting Information includes figures showing fabrication process of gold NR dimers and upright transmission spectroscopy and details of the measured and simulated results for gold ND dimers. This material is available free of charge via the Internet at http://pubs.acs.org.

■ AUTHOR INFORMATION

Corresponding Author

*E-mail: potsung@mail.nctu.edu.tw.

Notes

The authors declare no competing financial interest.

■ ACKNOWLEDGMENTS

This work is supported by Taiwan's National Science Council (NSC) under Contract Nos. NSC-100-2221-E-009-109-MY3 and NSC-100-2120-M-009-005-. The authors would like to thank the help from Center for Nano Science and Technology (CNST) at National Chiao Tung University (NCTU), Taiwan.

■ REFERENCES

(1) Barnes, W. L.; Dereux, A.; Ebbesen, T. W. *Nature* **2003**, *424*, 824−830.
(2) Ozbay, E. *Science* **2006**, *311*, 189−193.
(3) Lal, S.; Link, S.; Halas, N. J. *Nat. Photonics* **2007**, *1*, 641−648.
(4) Juan, M. L.; Righini, M.; Quidant, R. *Nat. Photonics* **2011**, *5*, 349−356.
(5) Wurtz, G. A.; Pollard, R.; Hendren, W.; Wiederrecht, G. P.; Gosztola, D. J.; Podolskiy, V. A.; Zayats, A. V. *Nat. Nanotechnol.* **2011**, *6*, 107−111.
(6) Aizpurua, J.; Bryant, G. W.; Richter, L. J.; García de Abajo, F. J. *Phys. Rev. B* **2005**, *71*, 235420.
(7) Gopinath, A.; Boriskina, S. V.; Premasiri, W. R.; Ziegler, L.; Reinhard, B. M.; Negro, L. D. *Nano Lett.* **2009**, *9*, 3922−3929.
(8) Theiss, J.; Pavaskar, P.; Echternach, P. M.; Muller, R. E.; Cronin, S. B. *Nano Lett.* **2010**, *10*, 2749−2754.
(9) Tripathy, S.; Marty, R.; Lin, V. K.; Teo, S. L.; Ye, E.; Arbouet, A.; Saviot, L.; Girard, C.; Han, M. Y.; Mlayah, A. *Nano Lett.* **2011**, *11*, 431−437.
(10) Wu, L.; Shi, C.; Tian, L.; Zhu, J. *J. Phys. Chem. C* **2008**, *112*, 319−323.
(11) Lee, S. Y.; Hung, L.; Lang, G. S.; Cornett, J. E.; Mayergoyz, I. D.; Rabin, O. *ACS Nano* **2010**, *4*, 5763−5772.
(12) Lin, V. K.; Teo, S. L.; Marty, R.; Arbouet, A.; Girard, C.; Alarcon-Llado, E.; Liu, S. H.; Han, M. Y.; Tripathy, S.; Mlayah, A. *Nanotechnology* **2010**, *21*, 305501.
(13) Pasquale, A. J.; Reinhard, B. M.; Negro, L. D. *ACS Nano* **2011**, *5*, 6578−6585.
(14) Hao, E.; Schatza, G. C. *J. Chem. Phys.* **2004**, *120*, 357−366.
(15) Angelis, F.; de; Patrini, M.; Das, G.; Maksymov, I.; Galli, M.; Businaro, L.; Andreani, L. C.; Fabrizio, E. D. *Nano Lett.* **2008**, *8*, 2321−2327.
(16) Li, Z. Y.; Xia, Y. *Nano Lett.* **2010**, *10*, 243−249.
(17) Mack, N. H.; Wackerly, J. Wm.; Malyarchuk, V.; Rogers, J. A.; Moore, J. S.; Nuzzo, R. G. *Nano Lett.* **2007**, *7*, 733−737.
(18) Su, Y. H.; Chang, S. H.; Teoh, L. G.; Chu, W. H.; Tu, S. L. *J. Phys. Chem. C* **2009**, *113*, 3923−3928.
(19) Juluri, B. K.; Chaturvedi, N.; Hao, Q.; Lu, M.; Velegol, D.; Jensen, L.; Huang, T. J. *ACS Nano* **2011**, *5*, 5838−5847.
(20) Su, K.-H.; Wei, Q.-H.; Zhang, X.; Mock, J. J.; Smith, D. R.; Schultz, S. *Nano Lett.* **2003**, *3*, 1087−1090.
(21) Lassiter, J. B.; Aizpurua, J.; Hernandez, L. I.; Brandl, D. W.; Romero, I.; Lal, S.; Hafner, J. H.; Nordlander, P.; Halas, N. J. *Nano Lett.* **2008**, *8*, 1212−1218.
(22) Funston, A. M.; Novo, C.; Davis, T. J.; Mulvaney, P. *Nano Lett.* **2009**, *9*, 1651−1658.
(23) Hatab, N. A.; Hsueh, C. H.; Gaddis, A. L.; Retterer, S. T.; Li, J. H.; Eres, G.; Zhang, Z.; Gu, B. *Nano Lett.* **2010**, *10*, 4952−4955.
(24) Rechberger, W.; Hohenau, A.; Leitner, A.; Krenn, J. R.; Lamprecht, B.; Aussenegg, F. R. *Opt. Commun.* **2003**, *220*, 137−141.
(25) Jain, P. K.; Huang, W.; El-Sayed, M. A. *Nano Lett.* **2007**, *7*, 2080−2088.
(26) Yang, S. C.; Kobori, H.; He, C. L.; Lin, M. H.; Chen, H. Y.; Li, C.; Kanehara, M.; Teranishi, T.; Gwo, S. *Nano Lett.* **2010**, *10*, 632−637.
(27) Prodan, E.; Radloff, C.; Halas, N. J.; Nordlander, P. *Science* **2003**, *302*, 419−422.
(28) Nordlander, P.; Oubre, C.; Prodan, E.; Li, K.; Stockman, M. I. *Nano Lett.* **2004**, *4*, 899−903.
(29) Aizpurua, J.; Hanarp, P.; Sutherland, D. S.; Käll, M.; Bryant, G. W.; García de Abajo, F. J. *Phys. Rev. Lett.* **2003**, *90*, 057401.
(30) Hao, F.; Larsson, E. M.; Ali, T. A.; Sutherland, D. S.; Nordlander, P. *Chem. Phys. Lett.* **2008**, *458*, 262−266.
(31) Banaee, M. G.; Crozier, K. B. *Opt. Lett.* **2010**, *35*, 760−762.
(32) Larsson, E. M.; Alegret, J.; Käll, M.; Sutherland, D. S. *Nano Lett.* **2007**, *7*, 1256−1263.
(33) Jung, K. Y.; Teixeira, F. L.; Reano, R. M. *J. Lightwave Technol.* **2007**, *25*, 2757−2765.
(34) Prodan, E.; Nordlander, P. *J. Chem. Phys.* **2004**, *120*, 5444−5454.
(35) Wu, Y.; Nordlander, P. *J. Chem. Phys.* **2006**, *125*, 124708.
(36) Wang, H.; Brandl, D. W.; Le, F.; Nordlander, P.; Halas, N. J. *Nano Lett.* **2006**, *6*, 827−832.
(37) Ye, J.; Dorpe, P. V.; Lagae, L.; Maes, G.; Borghs, G. *Nanotechnology* **2009**, *20*, 1−6.
(38) Gluodenis, M.; Foss, C. A. Jr. *J. Phys. Chem. B* **2002**, *106*, 9484−9489.
(39) Rakic, A. D.; Djurisic, A. B.; Elazar, J. M.; Majewski, M. L. *Appl. Opt.* **1998**, *37*, 5271−5283.

(40) Zhao, J.; Zhang, X. Y.; Yonzon, C. R.; Haes, A. J.; Van Duyne, R. P. *Nanomedicine* **2006**, *1*, 219−228.
(41) Anker, J. N.; Hall, W. P.; Lyandres, O.; Shah, N. C.; Zhao, J.; Van Duyne, R. P. *Nat. Mater.* **2008**, *7*, 442−453.
(42) Mayer, K. M.; Hafner, J. H. *Chem. Rev.* **2011**, *111*, 3828−3857.
(43) Liu, N.; Weiss, T.; Mesch, M.; Langguth, L.; Eigenthaler, U.; Hirscher, M.; Sonnichsen, C.; Giessen, H. *Nano Lett.* **2010**, *10*, 1103−1107.
(44) Nehl, C. L.; Liao, H. W.; Hafner, J. H. *Nano Lett.* **2006**, *6*, 683−688.